Synthesis, Crystal and Magnetic Structure of the New Double Perovskite Ba_2MnMoO_6

M. J. Martínez-Lope, J. A. Alonso, and M. T. Casais

Instituto de Ciencia de Materiales de Madrid, CSIC, Cantoblanco, E-28049 Madrid, Spain

Reprint requests to Dr. J. A. Alonso. E-mail: ja.alonso@icmm.csic.es

Z. Naturforsch **58b,** 571–576 (2003); received February 14, 2003

We describe the preparation and characterization of a new double perovskite of formula Ba_2MnMoO_6. It has been obtained in polycrystalline form by thermal treatment, in a H_2/N_2 flow, of previously decomposed citrate precursors. This material has been studied by X-ray (XRD) and neutron powder diffraction (NPD): it crystallizes, at room temperature, in the cubic space group $Fm\bar{3}m$, and shows an almost perfect ordering between Mn^{2+} and Mo^{6+} cations at the B substructure. Below T_N = 10.8 K, it experiences a long range antiferromagnetic ordering that was followed from sequential NPD data. The low-temperature magnetic structure is defined by the propagation vector **k** = (½, ½, ½). The ordered magnetic moment of Mn is found to be 4.04(8) μ_B at 2 K, suggesting a divalent oxidation state for Mn cations, in a high spin $t_{2g}^3e_g^2$ (S = 5/2) electronic configuration.

Key words: Perovskite Structure, Neutron Diffraction, Magnetic Structure, Antiferromagnetic Ordering, Manganese

Introduction

The discovery of colossal magnetoresistance (CMR) in manganese perovskites [1, 2] has renewed the interest in complex transition-metal oxides containing mixed valence ions, in the search for novel ferromagnetic and half-metallic oxides that can exhibit CMR. This interest led to the study of the so-called double perovskites, with general formula $A_2B'B''O_6$, where B′ and B″ sites are occupied alternately by different cations (transition metals) and A represents a rare-earth or alkaline-earth metal. The example of Sr_2FeMoO_6 [3, 4] with a Curie temperature (T_C) above room temperature (R.T.) and significant low-field magnetoresistance at R.T., has triggered the investigation of other double perovskites that could show similar or improved properties.

The ideal structure of these compounds can be viewed as a regular arrangement of corner-sharing $B'O_6$ and $B''O_6$ octahedra, alternating along the three directions of the crystal, with the voluminous A cations occupying the voids in between the octahedra. The crystal structure and physical properties of double-perovskite oxides depend considerably on the size and valences of the A, B′ and B″ cations. For instance, Sr_2FeMoO_6 is cubic ($Fm\bar{3}m$) above the ferromagnetic Curie temperature, and it undergoes a structural phase transition and becomes tetragonal ($I4/m$) below this temperature [5–7]. Ca_2FeMoO_6, Ca_2MnWO_6, Sr_2FeWO_6 are monoclinic ($P2_1/n$) with β angles very close to 90° [8–10].

The manganese analogues of A_2FeMoO_6 (A = Ca, Sr, Ba) have attracted our attention. In a previous report we have described the magnetic properties, crystal and magnetic structures of Sr_2MnMoO_6, Sr_2MnWO_6 and Ca_2MnWO_6 [9], all of them experiencing a low-temperature antiferromagnetic ordering. To the best of our knowledge, there are no reports on the preparation, crystal structure or physical properties of the Ba_2MnMoO_6 double perovskite. Other related manganese double perovskites exhibit a variety of magnetic structures, such as antiferromagnetic Ba_2MnWO_6 [11] or ferrimagnetic in Ba_2MnReO_6 [12, 13].

In the present work we describe the synthesis of Ba_2MnMoO_6, prepared by soft chemistry procedures, and the results of a neutron diffraction study on a well-crystallized sample, providing complete structural data for this perovskite. Low temperature NPD data allowed us to probe the microscopic origin of the antiferromagnetic ordering, and the evolution of the ordered Mn^{2+} magnetic moments.

0932–0776/03/0600–0571 $06.00

Experimental Section

Ba_2MnMoO_6 perovskite was prepared as a brown polycrystalline powder from citrate precursors obtained by soft chemistry procedures. Stoichiometric amounts of analytical grade $Ba(NO_3)_2$, $MnCO_3$ and $(NH_4)_6Mo_7O_{24}\cdot 4H_2O$ were dissolved in citric acid. The citrate and nitrate solution was slowly evaporated, leading to an organic resin containing a random distribution of the involved cations at an atomic level. This resin was first dried at 120 °C and then slowly decomposed at temperatures up to 600 °C. All the organic materials and nitrates were eliminated in a subsequent treatment at 800 °C in air for 2 h. This treatment gave rise to highly reactive precursor material. It was then treated in an H_2/N_2 (15%/85%) flow at 930 °C for 12 h.

The initial characterization of the product was carried out by X-ray diffraction (XRD) (Cu-K_α, λ = 1.5406 Å). Neutron powder diffraction (NPD) diagrams were collected at the Institut Laue-Langevin (ILL) in Grenoble (France). The crystallographic structure was refined from the high resolution NPD pattern, acquired at room temperature at the D2B diffractometer with λ = 1.594 Å. For the determination of the magnetic structure and the study of its thermal variation, a series of NPD patterns were obtained at the D20 high-flux diffractometer (ILL-Grenoble) with a wavelength of 2.42 Å, in the temperature range from 2 to 28 K. The refinements of the crystal and magnetic structure was performed by the Rietveld method, using the FULLPROF refinement program [14]. A pseudo-Voigt function was chosen to generate the line shape of the diffraction peaks. The coherent scattering lengths for Ba, Mn, Mo and O were 5.05, −3.73 , 6.72 and 5.803 fm, respectively.

Results

Ba_2MnMoO_6 was obtained as a well crystallized powder. The XRD diagram is shown in Fig. 1. The pattern is characteristic of a perovskite structure, showing superstructure peaks corresponding to the Mn/Mo ordering. No additional peaks or splitting of the reflections, which could have suggested a reduction in symmetry, were observed in the XRD pattern. It is worth commenting that the pure perovskite structure can only be obtained under reducing conditions, necessary to stabilize the Mn^{2+} cations. Treatments in air at increasing temperatures led to mixtures of oxides containing Mn^{2+}/Mn^{3+} mixed valences.

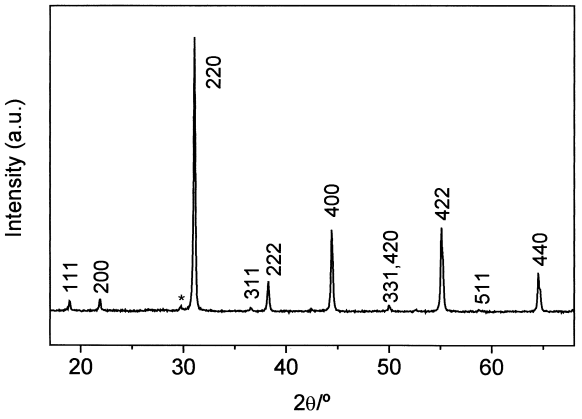

Fig. 1. XRD pattern of Ba_2MnMoO_6, indexed in a cubic unit cell with $\mathbf{a} = 2\mathbf{a}_0$, $\mathbf{a}_0 \approx 4$ Å. The star indicates the main reflection of an unidentified minor impurity phase.

Structural refinement

The structural refinement from R.T. high resolution NPD data was performed in the $Fm\bar{3}m$ space group (No. 225), Z = 4, with unit-cell parameters related to $\mathbf{a}_0$ (ideal cubic perovskite, $\mathbf{a}_0 \approx 3.9$ Å) as $\mathbf{a} = \mathbf{b} = \mathbf{c} = 2\mathbf{a}_0$. Ba atoms were located at the 8*c* position, Mn at 4*a*, Mo at 4*b*, and oxygen atoms at 24*e* site. An excellent fit was obtained for this model, as shown in Fig. 2. In the final refinement, the possibility of anti-site disordering was checked by assuming that some Mn atoms could occupy Mo sites, and *vice versa*. The refinement of the inversion degree led to less than 1% of antisite disordering. The oxygen content was also checked

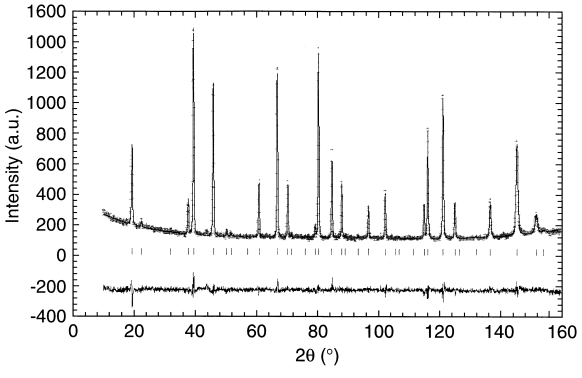

Fig. 2. Observed (crosses), calculated (full line) and difference (bottom) high resolution NPD Rietveld profiles for Ba_2MnMoO_6 at 295 K.

by refining its occupancy factors; no deficiency was detected within the standard deviations. The most important structural parameters of the crystallographic structure at R.T. and the discrepancy factors after the refinements are listed in Table 1. The main interatomic distances and angles are included in Table 2. A view of the crystal structure is shown in Fig. 3.

Magnetic structure

The magnetic structure of Ba_2MnMoO_6 and its thermal evolution was analysed using a set of NPD patterns collected in the temperature range $2 < T < 28$ K, with $\lambda = 2.42$ Å. As shown in Fig. 4, new reflections of magnetic origin appear on decreasing the temperature below 11 K, at positions forbidden for the Bragg reflections in the space group $Fm\bar{3}m$. These new peaks correspond to magnetic satellites defined by the propagation vector **k** = (½, ½, ½); the magnetic reflections are indexed in Fig. 4. An antiferromagnetic structure was modelled with magnetic moments at the Mn positions; the determination of the orientation of the moments is not possible in a cubic structure from powder data. We supposed that the moments are lying along the [0 0 1] direction. After the full refinement of the profile, including the magnetic moment magnitude, a discrepancy factor R_{mag} of 10.3% was reached for the 2 K diagram, collected

Table 1. Positional and displacement parameters for Ba_2MnMoO_6 in the cubic $Fm\bar{3}m$ space group, from NPD data at 295 K. Reliability factors after the Rietveld refinement are also given. The cubic unit-cell parameter is **a** = 8.18166(9) Å and V = 547.68(1) Å^3.

Atom	Site	*x*	*y*	*z*	B(Å^2)
Ba	8*c*	1/4	1/4	1/4	0.72(9)
Mn	4*a*	0	0	0	0.55(9)
Mo	4*b*	1/2	0	0	0.43(5)
O	24*e*	0.2640(3)	0	0	0.75(4)

Realiability factors: R_p (%) = 4.97, R_{wp} (%) = 6.32, R_{exp} (%) = 5.15, χ^2 = 1.51, R_I (%) = 3.84.

Table 2. Main bond lengths (Å) and selected angles (°) for cubic Ba_2MnMoO_6 determined from NPD data at 295 K.

Ba–O1 (×12)	2.895(2)	Mn–O1–Mo	180.0
Mn–O1 (×6)	2.160(2)	O1–Mn–O1	90.0
Mo–O1 (×6)	1.931(2)	O1–Mo–O1	90.0

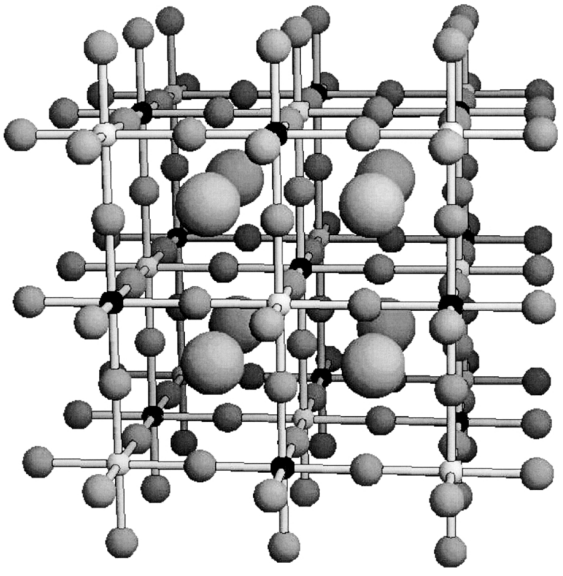

Fig. 3. A view of the crystal structure of the Ba_2MnMoO_6 double perovskite; each MnO_6 octahedron is linked to six MoO_6 octahedra.

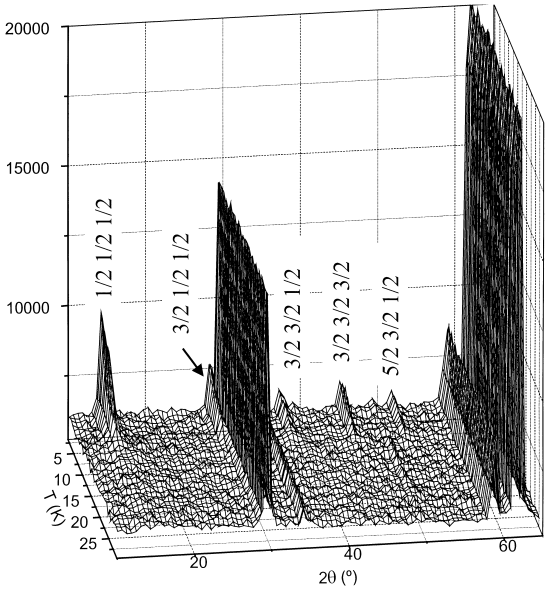

Fig. 4. Thermal evolution of the sequential NPD patterns, collected with $\lambda = 2.42$ Å. Below T_N, new reflections due to the establishment of a long-range magnetic ordering are observed.

with a good statistics. The magnetic structure is stable from 2 K to T_N, as demonstrated in a sequential refinement in the available temperature range. The thermal evolution of the magnetic moments on the Mn positions and the lattice parameter are shown in Fig. 5 and 6. The good agreement between the observed and calculated patterns at T = 2 K is illustrated in Fig. 7. The observed magnetic reflections are indexed in Fig. 7.

A view of the magnetic structure of Ba_2MnMoO_6 is displayed in Fig. 8. The magnetic arrangement can be described as a stacking of ferromagnetic layers of Mn moments perpendicular to the [1 1 1] direction, coupled antiferromagnetically from layer to layer.

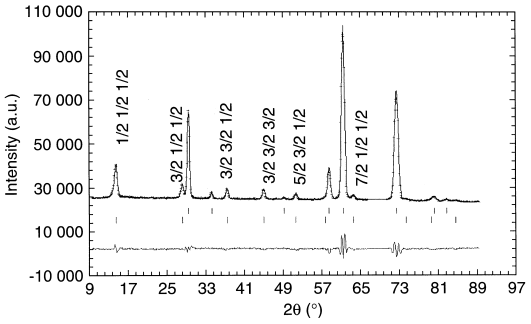

Fig. 7. Observed (solid circles), calculated (solid line) and difference (bottom line) NPD patterns collected at 2 K with λ = 2.42 Å. The two series of tick marks correspond to the crystallographic and magnetic Bragg reflections.

Discussion

The perovskite structure ABO_3 can be viewed as a network of corner-sharing BO_6 octahedra, with the A cations occupying the voids formed by these octahedra. If the size of A cations becomes small, the BO_6 octahedra tilt in order to optimise the A–O contacts. Ba_2MnMoO_6 adopts the well-known $(NH_4)_3FeF_6$ structure, in which MnO_6 and MoO_6 alternate along the three crystallographic directions. Given the large size of Ba^{2+} cations, the octahedral network is not tilted, keeping Mn–O–Mo angles at 180°. There is a perfect 1:1 B-site ordering, due to the large difference in charge existing between Mn^{2+} and Mo^{6+} cations. As shown in Table 2, the MnO_6 octahedra are larger than the MoO_6, an observation in accordance with the

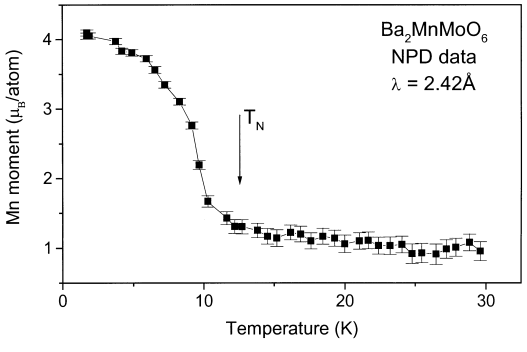

Fig. 5. Thermal variation of the ordered Mn magnetic moment for the antiferromagnetic structure for Ba_2MnMoO_6.

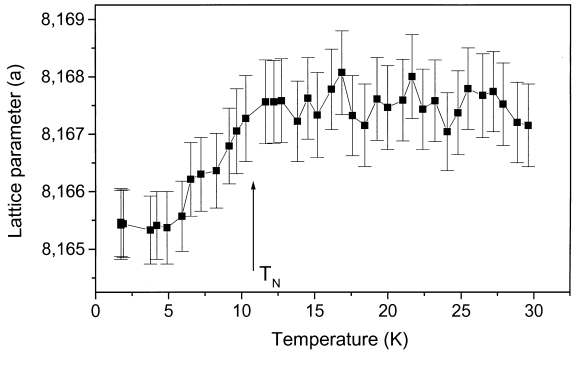

Fig. 6. Thermal dependence of the **a** unit-cell parameter for Ba_2MnMoO_6.

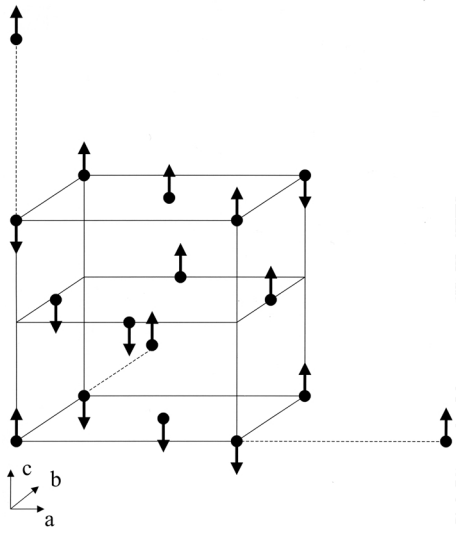

Fig. 8. A sketch of the magnetic structure for **k** = (½, ½, ½). For the sake of clarity, the figure shows the chemical cell (**a** ≈ 8 Å) and a part of three adjacent cells.

larger ionic radius of Mn^{2+} (r^{2+}_{Mn} = 0.97 Å) compared to Mo^{6+} (r^{6+}_{Mn} = 0. 73 Å) (15).

A bond valence calculation [16, 17] from the observed bond lengths can give some insight into the actual oxidation states of the different cations present in the crystal structure. In Ba_2MnMoO_6, the calculated valences for Ba, Mn and Mo are 2.34, 2.21 and 5.63 respectively. The Ba cation seems to be significantly overbonded, exhibiting a valence much higher than the expected 2+ value. In fact, the observed Ba–O distances are much shorter (Table 2) than expected from the sum of the ionic radii (3.01 Å). It seems that the much more covalent network determined by MnO_6 and MoO_6 octahedra mainly determines the size of the unit cell; the low degree of freedom of this cubic structure constrains the Ba–O bond-lengths outside of the optimal values. The valences for Mn and Mo cations suggest oxidations states of 2+ and 6+, respectively. From these values, the electronic configuration in this compound at 298 K is $Mn^{2+}(3d^5)$–$Mo^{6+}(4d^0)$. This electronic configuration, excluding the presence of a mixed valence at Mn atoms and implying an oxidation state +6 for Mo cations, accounts for the electrical insulating behavior and brown colored aspect of this sample.

The ordered magnetic moment obtained for Mn cations from the refinement of the magnetic structure at 2 K is 4.04(8) μ_B . This suggests a high spin configuration for the Mn^{2+} cations ($t^3_{2g}e^2_g$, S = 5/2). The reduction of the saturation moment with respect to the expected value of 5 μ_B is believed to be due to covalence effects. It is interesting to compare the Néel temperature of Ba_2MnMoO_6 (T_N = 11 K) with that recently reported for the related compound Sr_2MnMoO_6 [9], T_N = 15 K, implying the presence of stronger magnetic interactions for the strontium oxide. These interactions are certainly related to the significantly shorter Mn–O distances observed in Sr_2MnMoO_6, of 2.13 Å (for the Ba compound 2.16 Å), which account for a stronger overlap between Mn 3d and O 2p orbitals, thus enhancing the superexchange process giving rise to the establishment of the antiferromagnetic ordering. Another interesting comparison can be established with the related Ba_2MnWO_6 perovskite [11], exhibiting the same cubic crystal structure and Mn–O–W angles of 180°. The Néel temperature of the tungsten compound is 9 K, suggesting weaker superexchange interactions which can be correlated with the slightly longer Mn–O bond-lengths for this oxide, of 2.176 Å.

The thermal evolution of the **a** unit-cell parameter (Fig. 6) seems to indicate a contraction of the unit-cell size at the onset of the antiferromagnetic ordering. This effect suggests the possibility of a magneto-elastic coupling, which has already been described for other antiferromagntic double perovskites [18] .However, this effect is not common in magnetic oxides, unless the magnetic transition is associated with an electronic fluctuation which is responsible for the change in the metal-oxygen bond strength. A well-known example is that of the $RNiO_3$ perovskites [19], where particularly spectacular changes in the unit-cell parameters and the volume are experienced at the onset of the metal-insulator transition that these oxides exhibit as a function of temperature. The present magneto-volume effect suggests a subtle change in the electron localization concomitant with the antiferromagnetic ordering in the Ba_2MnMoO_6 perovskite.

Conclusions

The new Ba_2MnMoO_6 double perovskite was obtained under a reducing H_2/N_2 flow from citrate precursors. The study of the crystallographic structure using NPD data allowed us to establish that this double perovskite adopts a cubic structure, space group $Fm\bar{3}m$, **a** = 8.18166(9) Å. Below T_N = 10.8 K, it experiences a long range antiferromagnetic ordering. The magnetic structure is defined by the propagation vector **k** = (½, ½, ½) and consists of ferromagnetic [1 1 1] layers of Mn^{2+} moments coupled antiferromagnetically. The magnetic moment obtained from Rietveld refinement of 2 K data is 4.04(8) μ_B. It seems clear that only the Mn ions are concerned in the magnetic ordering, adopting a +2 oxidation state, in a high-spin configuration. We have found a correlation between the Mn–O bond lengths, responsible for the strength of the superexchange process, and the Néel temperature in other double perovskites with related compositions.

Acknowledgements

We thank the Spanish Ministry of Science and Technology for financial support under project MAT2001-0539, and we are grateful to ILL for making all facilities available.

[1] S. Jin, T. H. Tiefel, M. McCormack, R. A. Fastnacht, R. Ramesh, and L. H. Chen, Science **264**, 413 (1994).
[2] R. Von Hemlholt, J. Wecker, B. Holzapfel, L. Shultz, and K. Samwer, Phys. Rev. Lett. **71**, 2331 (1994).
[3] K. I. Kobayaski, T. Kimura, H. Sawada, K. Terakura, and Y. Tokura, Nature **395**, 677 (1998).
[4] K. Ueda, H. Tabata, and T. Kawai, Science **280**, 1064 (1998).
[5] F. K. Patterson, C. W. Moeller, and R. Ward, Inorg. Chem. **2**, 196 (1963).
[6] F. Galasso, F. Douglas, and R. J. Kasper, Chem. Phys. **44**, 1672 (1966).
[7] O. Chmaissen, R. Kruk, B. Dabrowski, D. E. Brown, X. Xiong, S. Kolesnik, J. D. Jorgensen, and C. W. Kimball, Phys. Rev B **62**, 197 (2000).
[8] J. A. Alonso, M. T. Casais, M. J. Martínez-Lope, J. L. Martínez, P. Velasco, A. Muñoz, and M. T. Fernández-Díaz, Chem. Mater. **12**, 161 (2000).
[9] A. Muñoz, J. A. Alonso, M. T. Casais, M. J. Martínez-Lope, and M. T. Fernández-Díaz, J. Phys.: Condens. Matter **14**, 8817 (2002).
[10] A. K. Azad, S. G. Eriksson, A. Mellergard, S. A. Ivanov, J. Eriksen, and H. Rundlöf, Mater. Res. Bull. **37**, 1797 (2002).
[11] A. K. Azad, S. A. Ivanov, S. G. Eriksson, J. Eriksen, H. Rundlöf, R. Mathieu, and P. Svedlinddh, Mater. Res. Bull. **36**, 2215 (2001).
[12] C. P. Khattak, D. E. Cox, and F. F. Y. Wang, J. Solid State Chem. **13**, 77 (1975).
[13] A. W. Sleight and J. F. Weither, J. Phys. Chem. Solids **33**, 679 (1972).
[14] J. Rodríguez-Carvajal, Physica B **192**, 55 (1993).
[15] R.D. Shannon, Acta Crystallogr. Sect. A **32**, 751 (1976).
[16] I. D. Brown, in M. O'Keefe and A. Navrotsky (eds): Structure and Bonding in Crystals, Vol. 2, p. 1, Academic Press, New York (1981).
[17] N. E. Brese and M. O'Keefe, Acta Crystallogr. Sect. B **47**, 192 (1991).
[18] M. J. Martínez-Lope, J. A. Alonso, M. T. Casais, and M. T. Fernández-Díaz, Eur. J. Inorg. Chem. 2463 (2002).
[19] J. L. García-Muñoz, J. Rodríguez-Carvajal, P. Lacorre, and J. B. Torrance, Phys. Rev. B **46**, 4414 (1992).